Advances in Nanochemistry
ISSN: 2676-5462

Research

Trace-level determination of trazodone with electrochemical sensor based on TiO_2-cMWCNTs nanocomposite

Mohammad Bagher Gholivand *, Zahra Godini

Department of Analytical Chemistry, Razi University, Kermanshah, Iran

Received 14th July 2021,
Accepted 15th October 2021,
DOI:10.22126/anc.2021.6694.1028

Abstract

The electrochemical oxidation of an antidepressants drug, trazodon (TRZ) on the modified titanium dioxide–carboxylated multiwall carbon nanotube glassy carbon electrode (TiO_2-cMWCNTs/GCE) was studied. The TiO_2-cMWCNTs/GCE sensor was characterized by scanning electron microscopy (SEM) and electrochemical impedance spectroscopy (EIS). The influence of the effective parameters on the electrochemical behavior of TRZ such as: pH, modifier volume, accumulation potential and time were optimized. Under the optimized conditions, the proposed sensor was applied to determine TRZ in the ranges of 6–100 nM and 100-1000 nM with the detection limit of 5 nM using differential pulse anodic stripping voltammetry (DPASV) at neutral pH. The modified electrode exhibited a good sensitivity, stability and pleasant reproducibility, which was also applied for the determination of TRZ in the spiked human serum and pharmaceutical formulations, with satisfactory results.

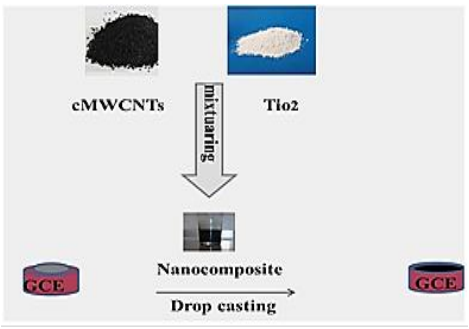

Keywords: *Trazodone, Titanium dioxide nanoparticles, Multi-walled carbon nanotubes, Modified electrode.*

Introduction

Trazodone,(2-{3-[4-(3-chlorophenyl)-1-piperazinyl}propyl]-1,2,4-triazole[4,3-a]pyridine-3(2H)-one hydrochloride, TRZ (Figure 1) is a weak inhibitor of monoamine reuptake and its major mechanism of action seems to be the antagonism at serotonin 5-HT_2/5-HT_{10} receptors.[1] TRZ is one of the second generation antidepressants,[2,3] and it's used for the treatment of major depression, sometimes in conjunction with selective serotonin reuptake inhibitors, like fluoxetine.[4] Unlike the tricyclic antidepressants, TRZ does not inhibit the peripheral reuptake of noradrenaline, although it may indirectly facilitate neuronal release. TRZ blocks central α_1-adrenoceptors and appears to have no effect on the central reuptake of dopamine.[5] Also TRZ is used to control sleep disturbance symptoms when using serotonin and norepinephrine reuptake inhibitors.[6] TRZ is mainly metabolized in the liver by the cytochrome isoform CYP_3A_4. The most important metabolite thus formed is 3-(1-clorophenyl) piperazine,[7] which was a serotonergic agonist with a long half-life.[8] TRZ is 85-95% protein-bound,[9-11] which means that tremendous change in pharmacology or adverse effects will occur when its relatively small a ''protein-unbound'' portion is altered. Serotonin syndrome may occur when TRZ is used in combination with other serotonergic agent such as nefazodone and venlafaxine.[12,13] The main side effects associated with TRZ administration are: nausea, insomnia, agitation, dry mouth, constipation, headache, hypotension, blurred vision, and confusion.[14] For these reasons, it was important to analyze TRZ in real samples.

Some methods have been reported for the determination of TRZ in pharmaceutical formulations or biological samples including spectrophotometry,[15] gas chromatography,[16] and high-performance liquid chromatography (HPLC).[17,18] Certain electrochemical studies have also been performed by polarography,[19] cyclic voltammetry, coulometry, and exhaustive electrolysis on the carbon paste electrode,[20] voltammetry by comparison with chromatography,[21] voltammetry using platinum electrode in rotating condition[22] and by using direct current, differential-pulse and alternating current polarography.[23] Although HPLC has been widely applied because of its high sensitivity and selectivity and the ability to minimize interferences, it is time consuming, solvent usage intensive and requires expensive devices and maintenance. Electrochemical detection of analytes is a very elegant method in analytical chemistry.[24] Carbon nanotubes (CNTs) have attracted increasing research interests due to their unique electrical, geometrical, and mechanical properties.[25] Moreover,

*Corresponding authors: Mohammad Bagher Gholivand, Email: mbgholivand2013@gmail.com

Cite this article: Gholivand, M.B. & Godini, Z. (2021). Determination trace level of trazodone with electrochemical sensor base on nanocomposite TiO_2-cMWCNTs/GC. *Advances in Nanochemistry*, 3(2), 88-96. DOI: 10.22126/anc.2021.6694.1028

Publisher: Razi University

CNTs coated with metal oxides are expected to exhibit different physical properties than those of neat CNTs. Recently, there is a considerable interest in using TiO_2 nanoparticles as a modifier since they have high surface area, optical transparency, good biocompatibility, and relatively good conductivity. The major barriers involve the low solubility of TiO_2 nanoparticles and the poor stability of the TiO_2 film on the electrode surface. Efforts have been made to obtain modified electrode with nano-TiO_2, e.g. screen printing procedure,[26] sol–gel strategy,[27] dispersing nano-TiO_2 with organic solvent,[28] and formation of hybrid film. In the last few years researchers have studied how to incorporate the CNTs into a metal oxide matrix, which results in hybrid films with good sensing function comparing with pure metal oxide sensors.[29-31] Two main reasons are generally accepted for the enhanced sensitivity found in CNT and metal oxide hybrid films. Increase of the surface area of CNTs-metal oxide hybrid films is known as the first reason. The second reason is due to the stretching of the depletion layer at the metal oxide grain boundaries as well as at the CNTs-metal oxide interface when the detected analytes are adsorbed.[32,33] However, to the best of our knowledge, electrochemical determination of TRZ using TiO_2 nanoparticles and CNTs has not been reported. The objective of the present work is to develop a convenient and sensitive method for the determination of TRZ based on the unusual properties of MWCNTs-modified electrode. Here, we report the electrochemical oxidation of TRZ on TiO_2-cMWCNTs modified glassy carbon electrode. The ability of the modified electrode for voltammetric response of the selected compound was evaluated. Finally, this modified electrode was used for the analysis of TRZ in pharmaceutical and serum samples. The resulted sensor exhibitshigh sensitivity, rapid response, good reproducibility and freedom of other potentially interfering species.

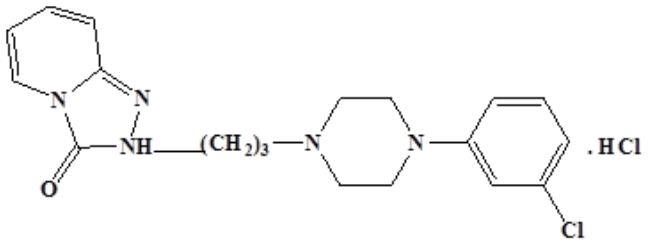

Figure 1. *Chemical structure of trazodone.*

Experimental

Reagents and chemicals

TRZ was obtained from sigma Aldrich F_w=408.32 ($C_{19}H_{22}ClN_5O.HCl$ >99% HPLC, Powder). A 1.0 mM stock solution was prepared in methanol and then stored in the dark at 25 °C. Carboxylated multiwalled carbon nanotubes (95%, 10-nm diameter, 1- to 2-mm length) were obtained from Dropsens (Lla-nera, Spain). 0.1 M phosphate buffer containing 0.1 M KCl with various pH values were prepared by mixing the stock solutions of Na_2HPO_4 and NaH_2PO_4, and adjusted by an appropriate amounts of hydrochloric acid or sodium hydroxide throughout the experiment. Double-distilled water was used throughout. All other chemicals were of analytical grade and were purchased from Merck (Darmstadt, Germany). All experiments were carried out at room temperature.

Apparatus

Electrochemical experiments were performed using a µAutolab III (Eco Chemie BV) potentiostat/galvanostat and the NOVA 1.8 software. A conventional three-electrode cell was used with a saturated SCE as the reference electrode, a Pt wire as the counter electrode, and a modified glassy carbon (1.8-mm diameter) as the working electrode. The cell was a one-compartment cell with an internal volume of 10 ml. A pH meter (Jenway, Model 3345) was used for pH measurements. To obtain information about the morphology of the electrode surface, scanning electron microscopy SEM; (TSCAN Co., Czech Republic), and X-ray diffractometry (X'Pert ProMPD, PANalytical, The Netherlands) were used.

Synthesis of TiO_2NPs

TiO_2NPs were synthesized according to the previously published report.[34] Briefly, TiO_2 nanoparticles were prepared by a sol–gel process of $Ti(OBu)_4$ in the presence of deionized water, ethanol, and HNO_3 under ultrasonic irradiation. In a typical process, 5 mL of $Ti(OBu)_4$ was dissolved in 5 mL anhydrous alcohol and ultrasonically dispersed to produce a mixture. Meanwhile, 5 mL of water and 1 mL of HNO_3 (65 %) were added to another 20 mL of absolute C_2H_5OH in turn to form an ethanol–nitric acid–water solution. The $Ti(OBu)_4$–C_2H_5OH solution was slowly added drop wise to the ethanol–nitric acid–water solution under ultrasonic irradiation in a sonication cell for 15 min to carry out a hydrolysis. Then, a semitransparent sol gel was gained after continuously sonication for 1 h. Subsequently, the sonication was conducted so that the temperature was raised from 25 to 80 °C at the end of the reaction. The obtained precipitates were separated by filtering, washing for several times with deionized water and anhydrous alcohol, drying at 70 °C in the air for about 12 h to produce dry gel powder after grinding. Finally, TiO_2 nanoparticles were obtained by calcining the dry gel precursor at 480 °C for 2 h in air, 50 nm.

Modification of GCE

The procedure of the fabrication of the sensor is illustrated in Scheme 1. To prepare a modified electrode, glassy carbon electrode was polished with emery paper followed by alumina (0.05 µm) and then thoroughly washed with double distilled water. Then it was sonicated in ethanol and distilled water for 20 minutes to remove adsorbed particles. Then 6 µL of above solution was dropped on the cleaned GC electrode surface to construct the TiO_2-cMWCNTs/GC electrode and then it was dried at room temperature to obtain the modified electrode. Finally, the electrode was rinsed carefully with double-distilled water and used for subsequent experiments.

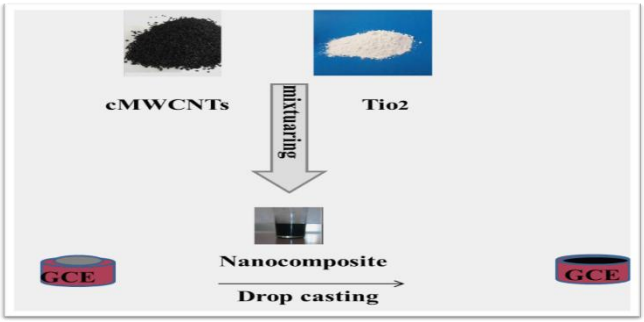

Scheme 1. *The procedure of the sensor fabrication.*

Analytical procedure

10 mL phosphate buffer solution (PBS), with pH 7.0, was transferred in to the voltammetric cell. An accumulation potential of 100 mV was applied to the electrode for 120 s while the solution was stirred at 400 rpm. The stirring was then stopped for a period of 10 s (equilibration time), and then its differential pulse voltammogram was recorded by scanning the potential from 0.5 to 0.9 V and was used for background correction. Then, an appropriate volumes of

the sample solution were added to the content of the cell and the same procedure was used for recording of their voltammograms for construction of calibration curve. After each experiment, the electrode was washed with double-distilled water and the PBS buffer solution (pH 7.0).

Real samples preparation

The contents of five TRZ tablets, each tablet containing 100 mg TRZ, were weighed and ground to a homogeneous fine powder in a mortar. The appropriate amount of the fine powder was dissolved in methanol to achieve a final concentration of 100 µM. After 20 min sonication of the mixture, it was filtered by passing through No. 1 filter paper and then diluted to volume with phosphate buffer solution (pH 7). Finally, the proposed procedure was used for monitoring the TRZ presented in the solution.

Serum samples, obtained from healthy volunteers were stored frozen until assay. An aliquot 0.5 mL methanol, as serum protein denaturation and precipitating agent, was added to 1 mL of the serum sample. After vortexing for 40 s, the precipitated protein was separated out by centrifugation for 4 min at 4,000 rpm. The clear supernatant layer was filtered through a 0.45 µm Millipore filter to produce a protein-free human serum. The serum sample was diluted 100 times with PBS (pH 7.0) solution without any further pretreatment.

Results and discussion

Characterization of Nanoparticles

In Figure 2, X-ray power diffraction analysis method was employed to investigate the formation of the TiO_2 nanoparticle. As for the TiO_2 nanoparticle, the peaks at 2θ values of ca. 25.2°, 37.8°, 48°, 54.7°, and 62.6° could be assigned the (101), (004), (200), (105), (211), and (204) planes of anatase TiO_2, suggesting the formation of anatase TiO_2 nanoparticles. Eventually, SEM was used in order to investigate the morphology of the TiO_2NPs. As can be seen clearly in Figure 3, the morphology of the particles is close to sphere.[35]

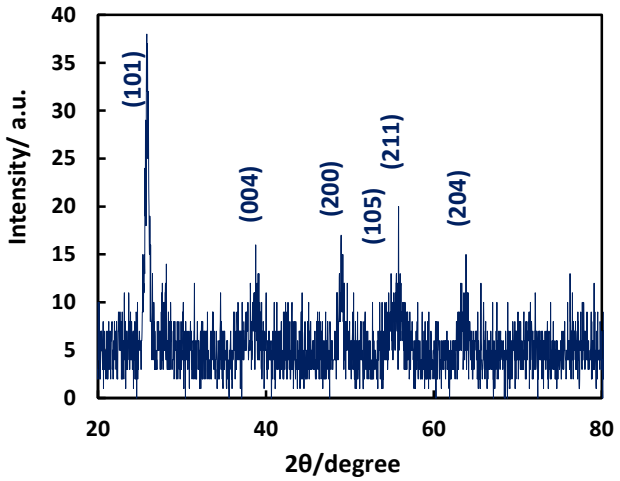

Figure 2. *XRD patterns of the TiO_2 nanoparticle.*

Characterization of modified electrode

Scanning electron microscopy (SEM) was used to study the surface morphology of the modified electrode. Figure 3 presents the SEM images of GCE (A), cMWCNTs/GCE (B), and TiO_2-cMWCNTs/GCE (C). The morphology of bare GCE (Figure 3A) reveals a smooth and homogeneous surface, characterized by the presence of polishing streaks. The cMWCNTs/GCE (Figure 3B) exhibits a homogenous structure without aggregation that was evenly coated on the surface of the electrodes. After coating the TiO_2-cMWCNTs on GC electrode, the morphology of the electrode surface was obviously changed indicating that the TiO_2-cMWCNTs immobilized onto GCE (Figure 3C). The results confirm the successful preparation, which could be applied to further uses.

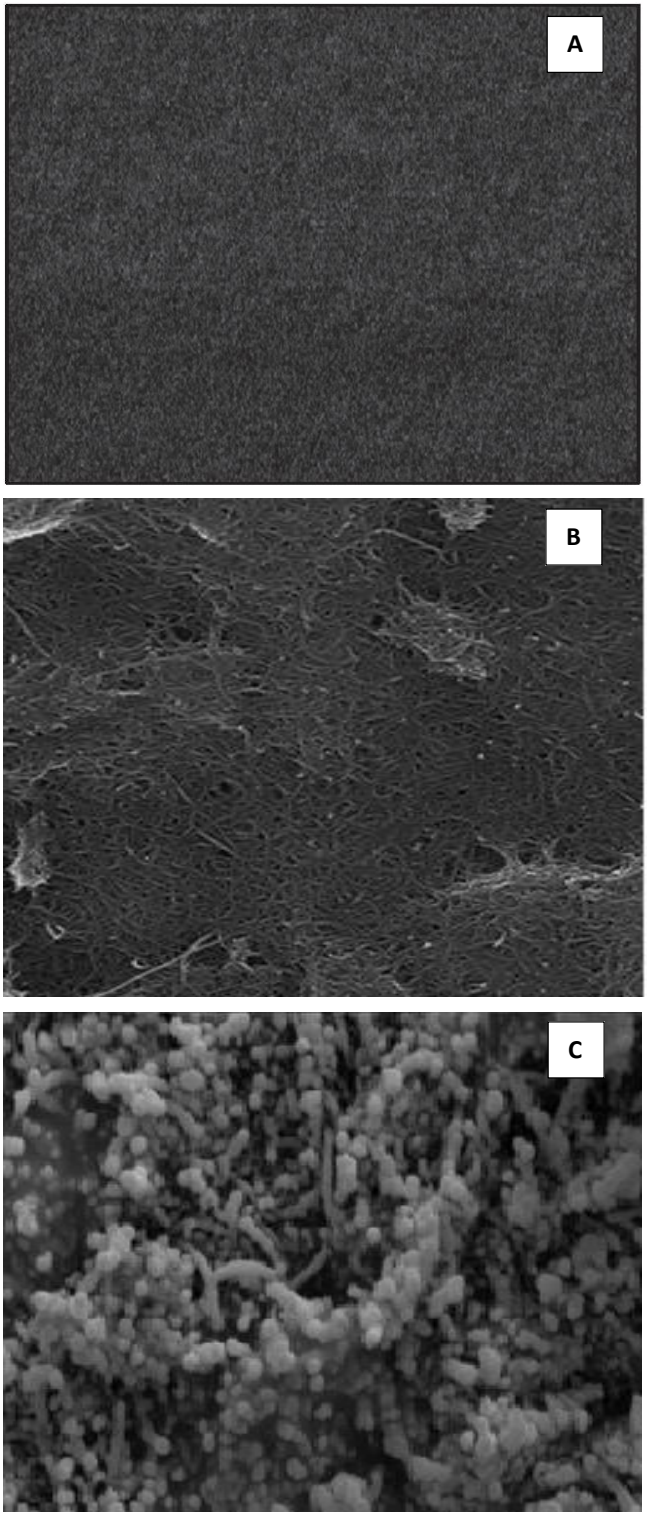

Figure 3. *SEM images of **(A)** GCE, **(B)** cMWCNTs/GCE, and **(C)** TiO_2-cMWCNTs/GCE samples.*

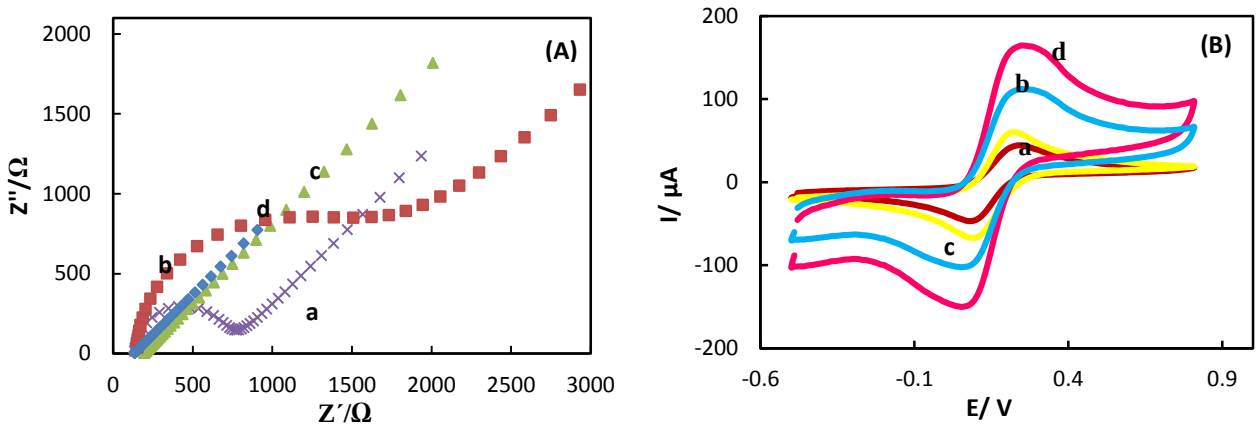

Figure 4. (A) *Nyquist plots of the different electrodes in a 1 mM $K_3[Fe(CN)_6]/K_4[Fe(CN)_6]$ 0.1 M KCl solution. (a) GCE, (b) TiO_2, (c) cMWCNTs, and (d) TiO_2-cMWCNTs/GCE.* ***(B)*** *The CV response of (a) GCE, (b) TiO_2/GCE, (c) cMWCNTs/GCE, and (d) TiO_2-cMWCNTs/GCE, in 1 mM $K_3[Fe(CN)_6]/K_4[Fe(CN)_6]$ 0.1 M KCl solution at scan rate of 100 mVs^{-1}.*

Electrochemical impedance spectroscopy (EIS) can also provide a useful information about changes of the electrode surface during the fabrication process. The electron-transfer resistance (R_{et}) at the electrode surface is equal to the semicircle diameter of the Nyquist plots and can be used to describe the interface properties of the electrode. Figure 4A shows the plots recorded in 0.1 M KCl containing 5 mM $[Fe(CN)_6]^{3-/4-}$ as the probe for bare GCE (curve a), cMWCNTs/GCE (curve b), TiO_2/GCE (curve c), and TiO_2-cMWNTs/GCE (curve d). The electron transfer resistance (R_{et}) at the bare GCE was 603 Ω which was decreases to 134 Ω after modification of the GCE with cMWCNTs (curve b). These results suggest that MWCNTs promotes the electron transfer of the electrodic process.

When the GCE was modified with TiO_2 (curve c), the R_{et} increased (R_{et}=1500 Ω) that may be due to presence of TiO_2 as a semiconductor[36] which reduces the arrival of the redox probe ($[Fe(CN)_6]^{3-/4-}$) to the electrode surface by electrostatic repulsive force (curve c). Finally, after modification of GCE with TiO_2-cMWNTs/GCE, the R_{et} was reduced to 127 Ω which is smaller than those of the tested electrodes (curve d). However, on the immobilization of TiO_2NPs into cMWCNTs, the semicircle part of the electrode further decreases. Decreasing in the charge transfer resistance is in line with the coating of the surface of GCE, confirming the creation of a new layer on the surface of the electrode and this proves that TiO_2NPs present in cMWCNTs film enhance electron between the reactant and electrode surface.

$[Fe(CN)_6]^{3-/4-}$ are valuable and convenient probe to characterize the electrochemical performance of the modified electrodes. Figure 4 indicates the cyclic voltammograms of 5.0 mM $[Fe(CN)_6]^{3-/4-}$ in 0.1 M KCl solution at the bare GCE (curve a), cMWCNTs/GCE (curve b), TiO_2/GCE (curve c) and TiO_2-cMWNTs/GCE (curve d). As it is seen at the all tested electrodes a redox peaks due to oxidation and reduction of the probe was appeared with different peaks current. The peaks current of the probe were increased when the GCE was modified by cMWCNTs it as an excellent conductive nanoparticle that can increases the electron transfer at the surface of the electrode. When TiO_2-cMWNTs was used as nanocomposite modifier (curve e) confirming the creation of nanocomposite on the electrode surface that enhances the electron transfer between the reactant and electrode surface. In the case TiO_2/GCE (curve c) the peaks current of the probe reduced relative to those of cMWCNTs/GCE and TiO_2-cMWNTs/GCE which confirmed the results of EIS.

Cyclic voltammetric behavior of TRZ

The electrochemical behaviors of TRZ at the surface of GCE, TiO_2/GCE, cMWCNTs/GCE, and TiO_2-cMWCNTs/GCE was investigated using cyclic voltammetry and the results are depicted in Figure 5. As can be seen, 3 µM TRZ in PBS at pH 7.0 showed an irreversible oxidation peak at the bare GCE (Figure 5, curve a), revealing that the oxidation activity of TRZ on GCE surface is poor. However, this anodic peak was decreased when GCE was modified by TiO_2 modifier (curve b) that may be due to enhancement in the charge transfer resistance of the resulted electrode in the presence of TiO_2 as a semiconductor which confirmed the EIS results.

Modification of the bare GCE by cMWCNTs increases the anodic peak current of TRZ that may be due to increasing the surface area and facilitating the electron transfer process (curve c). Finally, by immobilizing of the nanocomposite of TiO_2-cMWNTs on the GCE, the oxidation signal of TRZ greatly increased which exhibiting the effect of the last modifier toward the oxidation of TRZ (curve d). The remarkably enhancement in the sensitivity to the TRZ made the TiO_2-cMWCNTs/GC electrode as a suitable sensor for monitoring of this drug

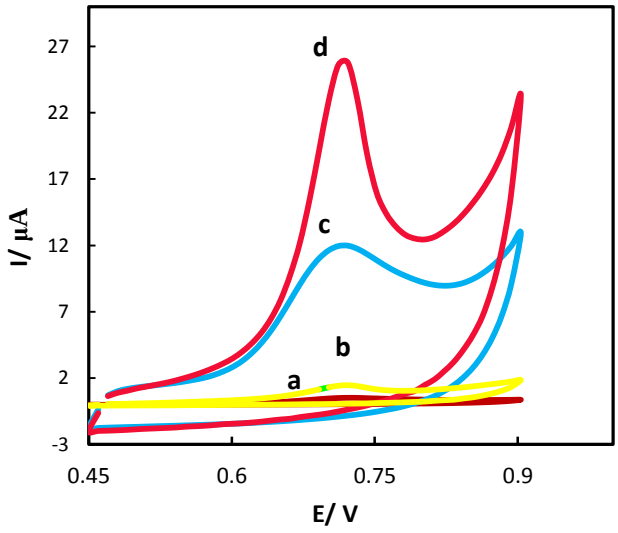

Figure 5. *Cyclic voltammograms of 3 µM of TRZ at (a) GCE, (b) TiO_2/GCE, (c) cMWCTs/GC, and (d) TiO_2-cMWCNTs/GCE; measurement conditions: pH 7.0, scan rate = 100 mVs^{-1}.*

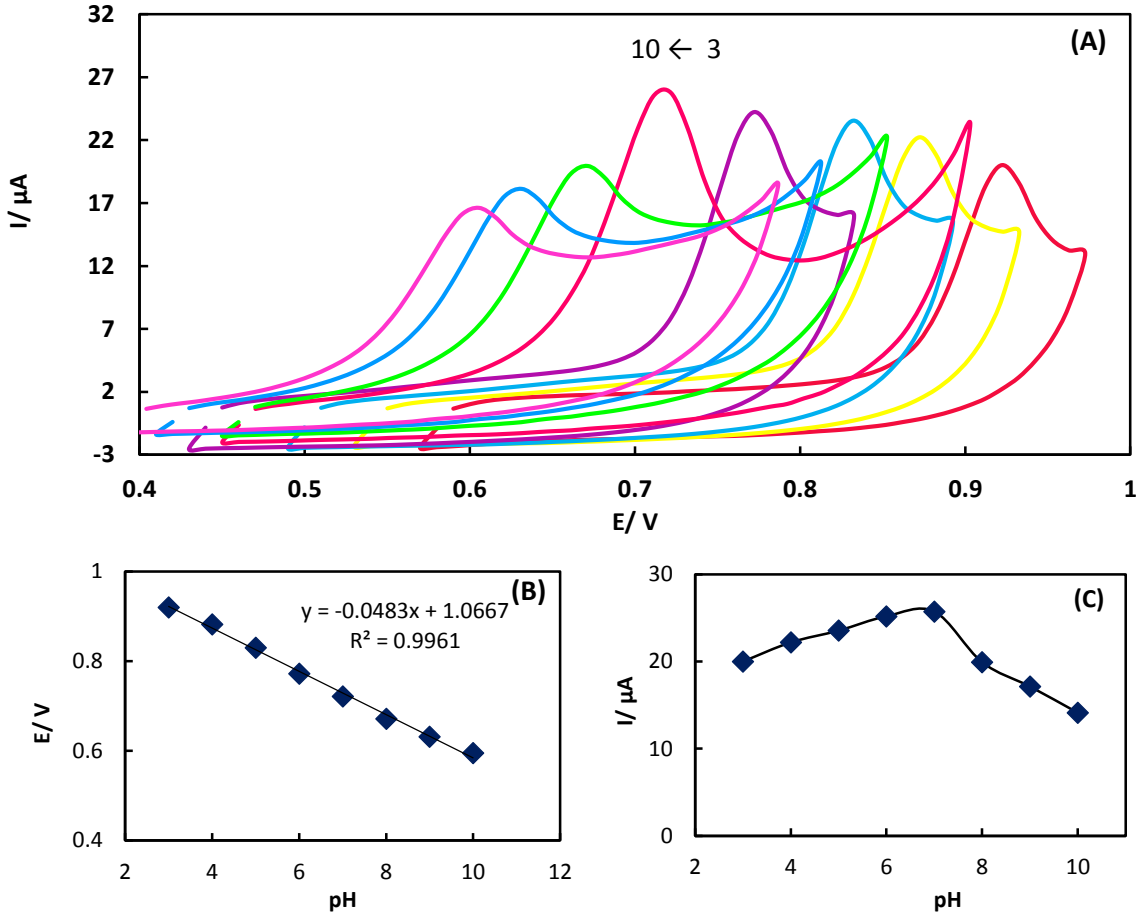

***Figure 6**. Effect of pH on the shape of 3 µM TRZ at in phosphate buffers (PH=3-10), **(A)** blank CVs of TiO_2-cMWCNTs modified GCE; (pH:3-10) , scan rate = 100 mVs^{-1}, **(B)** variations of peak currents I_p/µA of TRZ with pH, and **(C)** the influence of pH on the peak potential E_p/V of TRZ.*

pH dependence study

The electrochemical behavior of TRZ was investigated at different pH values in the range 3.0-11.0 using the TiO_2-cMWNTs and the results are summarized in Figure 6A. The pH of the supporting electrolyte exerts a significant influence on the electrooxidation behavior of TRZ at the modified electrode. It was found that the peak current increases with pH rising, and it reaches a maximum at pH 7.0. Further increase in pH value, decreases the response of the electrode (Figure 6B). Furthermore, the peak potential (E_{pa}) shift towards the negative direction during the pH rising which also indicating the participation of the H^+ ions in the electrode reaction. Basically, two linear regions were obtained, one between pH 3.0 and 7.0 with a slope of 51 mV/pH and another between pH 7.0 and 10 with a slope 38 mV/pH. The intersection of the curves is located around pH 7, which was close to the pK_a of the piperazine moiety.[37] The obtained regression equations are $E_P(V) = - 0.0509\ pH + 1.797$ with $R^2 = 0.997$, and $E_P(V) = -0.038\ pH + 0.9751$ with $R^2 = 0.999$ (Figure 6C). For TiO_2-cMWCNTs/GCE, the slope of -51 mV/pH, indicates that the number of transferred protons and electrons involved in the oxidation of TRZ is equal.[39] The first trend corresponds to the conditions where the molecule is oxidized in its mono-protonated form. The positive charge of the drug at pH = 7 facilitates its accumulation at the negative charge surface of TiO_2-cMWCNTs/GCE.

***Table 1.** Comparison of some analytical characteristics of the proposed sensor with those of other electrochemical methods reported for the determination of TRZ.*

Determination method	Linear range (nM)	LOD (nM)	Reference
Platinum electrode (stationary)	10000-50000	2500	[22]
Platinum electrode (rotating)	10000-50000	1700	[22]
Dropping mercury electrode	800-2400	7397	[23]
MWCNT-modified GCE	200-10000	24	[38]
TiO_2-cMWCNTs/ GCE	6-100	5.6	This work

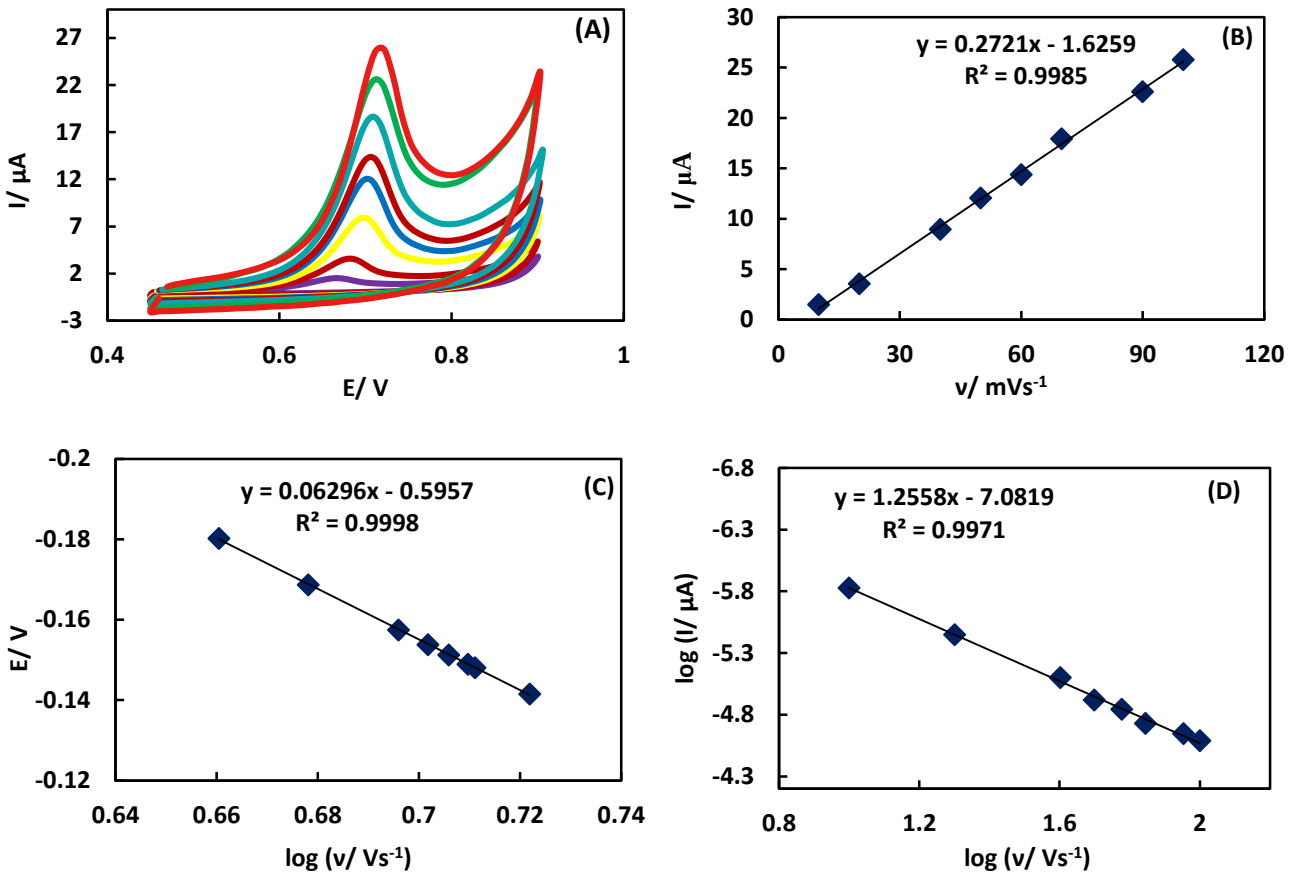

Figure 7. (A) *Cyclic voltammograms of the modified electrode in the presence of 1µM TRZ; at various scan rates, 10-100 mV s⁻¹.* ***(B)*** *The variation of peak current vs. scan rate,* ***(C)*** *the variation of logarithm of peak current and logarithm of scan rate,* ***(D)*** *the variation of oxidation peak potential vs. the logarithm of scan rate.*

Effect of scan rate

Also the effect of scan rate on the response of the TiO_2-cMWCNTs/GCE immersed in solution containing of 3 µM of TRZ was studied and its cyclic voltammograms are summarized in Figure 7. The peak current for the oxidation of TRZ is proportional to the scan rate (υ) in the range of 10–100 mVs^{-1} (Figure 7B), indicating that the oxidation of TRZ is adsorption-controlled. This mechanism was confirmed by plotting the log I_p vs. logυ (Figure 7D). The results also exhibited the variation of the logarithm of peak current (log I_p) with logarithm of scan rates (logυ). The linear equation of TRZ was logI_p = 1.2558 log υ – 7.0819; R^2= 0.9971. The slope of 1.2558 which is close to the theoretical value clearly indicates an adsorption-controlled electrode process. Furthermore, the peak potential also shifted to a more positive value with increasing the scan rate indicating the irreversibility of the electrooxidation of TRZ. According to Lavirone equation,[40-42] the linear relationship between peak potential (E_p) and logarithm of scan rate for an irreversible electrode process defines by the following equation:

$$E_p = E° + \left(\frac{2.303RT}{\alpha nF}\right) \text{Log}\left(\frac{RTK°}{\alpha nF}\right) + \left(\frac{2.303RT}{\alpha nF}\right) \log \upsilon \quad (1)$$

where α is the charge-transfer coefficient, k° the standard rate constant of the reaction, n the number of electrons transferred, v the scan rate, and other symbols have their usual meanings. The value of αn can be easily calculated from the slope of E_p–log v (Figure 7C) and it was found to be 0.938 at 25 °C. α is assumed to be 0.5 in a total irreversible electrode process. Therefore, the number of electrons (n) transferred in the electrooxidation of TRZ was calculated to be 1.876~2 which confirmed the proposed mechanism of TRZ oxidation[43] which was located on the piperazine moiety (Scheme 2).

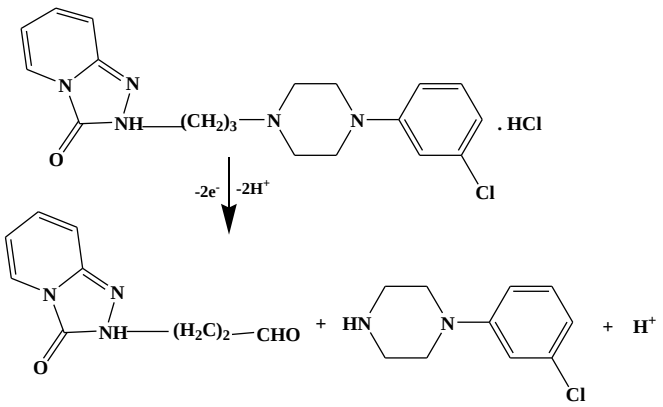

Scheme 2. *The proposed mechanism of TRZ oxidation.*

Optimization of parameters for TRZ detection

Effect of amount of modifier

The influence of immobilized TiO_2-cMWNTs/GCE modifier quantities onto the peak current response of TRZ was investigated. For this purpose different volumes of the TiO_2-cMWNTs/GCE

modifier were cast on the electrode surface. It was observed that by increasing the volume of suspension of TiO_2-cMWNTs modifier increases the peak current of 3 µM of TRZ up to 6 µL and then leveled off by further raising in volume of the suspention (Figure 8). Thus it is concluded that the optimum amount of TiO_2-cMWNTs/GCE modifier required to catalyze the oxidation of TRZ is 6 µL.

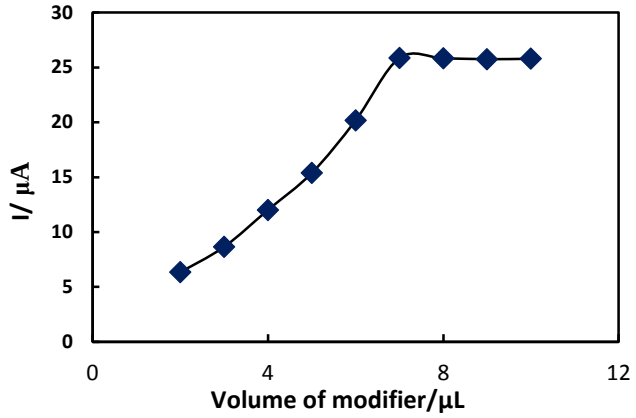

***Figure 8**. Influence of TiO_2-cMWCNTs/GCE nanocomposite volume used on the anodic peak current.*

Influence of accumulation potential and time

To increase the sensitivity of the TiO_2-cMWNTs/GCE for detection of TRZ, the differential pulse anodic stripping voltammetry (DPSV) as a sensitive was used. Accumulation potential is an important parameter for stripping techniques and has a non-negligible impact on the sensitivity of determination. The effect of accumulation potential on the oxidation peak currents of PBS (pH=7.0) containing 3 µM TRZ was examined over the potential range of -0.5 to 0.5 V. The oxidation peak currents increased up to 0.1 V, and then decreased. Thus, an accumulation potential of 0.1 V was chosen for subsequent use.

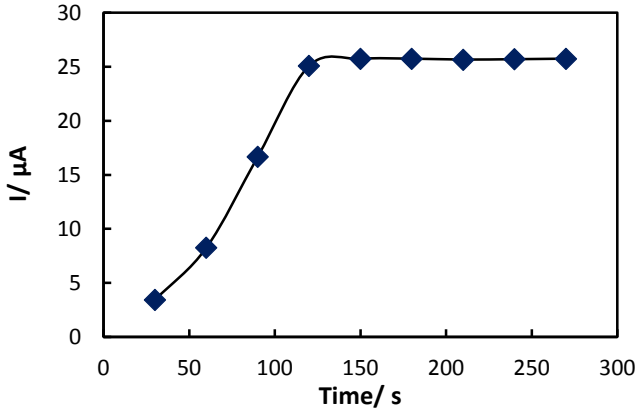

***Figure 9**. Variation of the anodic peak in DPSV test with accumulation time for 3 µM of TRZ.*

The influence of accumulation time on the response of the sensor was also investigated (Figure 9). Variations of the accumulation time in the range of 30 to 240 s showed that the peak currents of TRZ increased gradually with increasing accumulation times from 30 s to 120 s and then leveled off. This may be due to saturation of the electrode surface. So, 120 s was selected as the optimal accumulation time for subsequent uses. Afterward, the effects of stirring rate during the preconcentration period were also tested in the range 50 to 1000 rpm. The best results was obtained when 400 rpm was selected as optimal for the stirring rate.

Calibration curve

Under the optimum conditions the peak current of different amounts TRZ was used for plotting the calibration curve using DPSV. The DPSV voltammograms were recorded at accumulation potential (E_{ac}) of 0.1 V and the results after accumulation time of 120 s are presented in Figure 10A. Two linear relationships were obtained over TRZ concentrations ranges of 6 – 100 nM and 100 nM - 1000 nM (Figure 10B and C) The linear regression equations are:

$$I_P(\mu A) = 0.0000007 + 58.277C_{TRZ}(\mu M) \quad (R^2 = 0.9983) \qquad (2)$$

$$I_P(\mu A) = 0.000006 + 3.93624C_{TRZ}(\mu M) \quad (R^2 = 0.9914) \qquad (3)$$

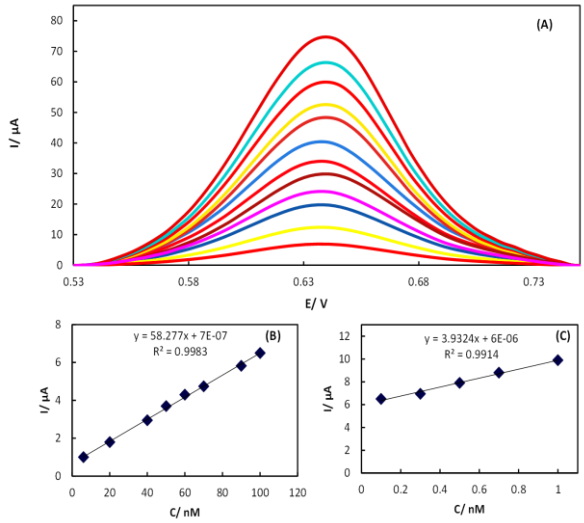

***Figure 10. (A)** Different pulse voltammogram of TiO_2-cMWCNTs/GCE in TRZ solution at different concentration and two linear rang plot of the peak current Ip/µA against the concentration: **(B)** 6-100 nM and **(C)** 100– 1000.*

The limit of detection (LOD) and limit of quantification (LOQ) were calculated using the relation ks/m,[20,22,23] where k=3 for LOD and 10 for LOQ, s represents the standard deviation of the peak currents of the blank (n = 10), and m represents the slope of the first calibration curve for TRZ. The LOD and LOQ values were found to

***Table 2.** Voltammetric determination of TRZ in real samples and recovery data obtained (n= 3).*

Sample	Added (µM)	Found (µM)	Recovery (%)	RSD (%)
Tablet	0.5	0.493	98.6	2.6
	0.1	0.101	101.0	3.2
Serum	0.5	0.516	103.2	3.5
	0.1	0.098	98.0	2.8

be 5.6 and 18.66 nM, indicating the suitability of the proposed modified electrode as a high sensitive sensor. Detection limit and linear range of the proposed electrode were compared with other previously reported methods, and the results were summarized in Table 1. As it can be seen, the linear range and LOD of the proposed method are comparable or better than those of other reports for TRZ determination.

When the concentration of TRZ was controlled at 3 µM, a good repeatability with relative standard deviation (R.S.D.) of 2.6% for five consecutive detections was observed. This level of precision is suitable for the TRZ quality control analysis of the drug in pharmaceutical dosage form and biological fluids. The sensor retained a response of 98.5% of the initial current after 30 days storage at room temperature, and it showed no obvious decline after use for 20 times. Reproducibility of proposed electrode was investigated by using DPSV. Five freshly electrodes were prepared on five consecutive days and the peak current of a solution containing 3 µM of TRZ was measured for each electrode. The relative standard deviation of peak currents was less than 3.1% which showed the reproducibility of the modified electrode.

Real sample analysis

To investigate the applicability of the proposed sensor to monitor TRZ in real samples, the TRZ in tablet and serum samples were measured by a standard addition method. The results are summarized in Table 2. As illustrated, the recovery of TRZ was between 98.0 and 103.2% using the TiO_2-cMWNTs/GCE. The results demonstrate the capability of the proposed sensor for the accurate voltammetric determination of ACV in real samples.

Interference

The influence of various substances as interfering compounds on the TRZ detection was studied under optimum conditions. Some common substances in pharmaceutical and/or in biological fluids were tested on the determination of the 0.1 µM TRZ. Tolerance limit was defined as the maximum concentration of the interfering substance that caused an error less than ±5% for the TRZ detection. The results showed that 500-fold of Ca^{2+}, Mg^{2+}, K^+, NH_4^+, SO_4^{2-}, Cl^-, and NO_3^-, 200-fold of glucose, sucrose, fructose, sorbitol, citric acid, uric acid, starch, and gelatin; and 100-fold of alanine, leucine, glycine, methionine, cysteine, and starch did not affect the selectivity. These results showed that the selectivity of the method is acceptable and it is suitable for the analysis of TRZ in real samples with different matrices.

Conclusion

In this study, a sensitive and selective voltammetric sensor based on a glassy carbon electrode modified with nanocomposite TiO_2-cMWNTs/GCE was fabricated. The modified electrode can be used for electrochemical investigation and the determination of TRZ. The TiO_2-cMWNTs/GCE modified electrode effectively facilitates both the adsorption of TRZ to the surface of electrode and the electron transfer in the electrooxidation of TRZ and its results was higher sensitivity. The performance of the proposed modified electrode in terms of limit of detection, and linear calibration range was compared with other reported TRZ sensors and the results are presented in Table 1. As it is seen this sensor is more sensitive than other work. Stability, repeatability and reproducibility are the other advantages the proposed modified electrode.

Acknowledgment

The authors gratefully acknowledge the financial support of this work by the Research Center of Razi University.

References

1. G.J. Marek, C.J. Mc Dougle, L.H. Price, and L.S. Seiden, *Psychopharmacology*, 109, **1992**, 2.
2. S. Rotzinger, M. Bourin, Y. Akimoto, R.T. Coutts, and G.B. Baker, *Cell. Mol. Neurobiol.*, 19, **1999**, 427.
3. S. Rotzinger, J. Fang, and G.B. Baker, *Drug Metab. Dispos.*, 26, **1998**, 572.
4. M. Maes, E. Vandoolaeghe, and R. Desnyder, J. *Affect Disorders*, 41, **1996**, 201.
5. K. Partill (Ed.), Martindale, The Complete Drug Reference, 32nd ed., The Pharmaceutical Press, (1999) Massachusetts, United States.
6. G. Bertschy, E. Ragama-Pardos, M. Muscinico, A. Ait-Ameur, L. Roth, C. Osiek, and F. Ferrero, *Pharm. Res.*, 51, **2005**, 79.
7. S. Rotzinger, J. Fang, and G.B. Baker, *Drug Metab. Dispos*., 26, **1998**, 572.
8. N. Samad, M.A. Haleem, and D.J. Haleem, *J. Chem. Soc. Pakistan*, 28, **2006**, 605.
9. B.N. Patel, N. Sharma, M. Sanyal, and P.S. Shrivastav, *J. Chromatogr. B:Anal. Technol. Biomed. Life Sci,* 871, **2008**, 44.
10. K.E. Thummel, D.D.S.N. Isoherranen, and H.E. Smith, Appendix II. Design and optimization of dosage regimens: pharmacokinetic data, in: L.L. Brunton, J.S. Lazo, K.L. Parker (Eds.), Goodman & Gilman's The Pharmacological Basis of Therapeutics, McGraw-Hill, Inc., (2006) New York, United States.
11. R. Venkataramanan, V. Ramachandran, B.J. Komoroski, S. Zhang, P.L. Schiff, and S.C. Strom, *Drug Metab. Dispos*., 28, **2000**, 1270.
12. H.C. Margloese and G. Chouinard, *Am. J. Psychiatr*., 157, **2000**, 1022.
13. R.E. McCue and M. Joseph, *Am. J. Psychiatr*., 158, **2001**, 2088.
14. S.C. Sweetman (Ed.),Martindale, The Complete Drug Reference, 34th ed., Pharmaceutical Press, (2004) London, United Kingdom.
15. S.N. Dhumal, P.M. Dikshit, I.I. Ubharay, B.M.Mascarenhas, and C.D. Gaitonde, *Indian Drugs*, 28, **1991**, 565.
16. A.J.H. Louter, R.A.C.A. Vander Wagt, and U.A.T. Brinkman, *Chromatographia*, 40, **1995**, 500.
17. X. Kang, C. Pan, Q. Xu, Y. Yao, Y.Wang, D. Qi, and Z. Gu, *Anal. Chim. Acta*, 587, **2007**, 75.
18. A. de Castro, M.M.R. Fernadez, M. Laloup, N. Samyn, G. De Boeck, M. Wood, V.Maes, and M. lopez-RIvadulla, *J. Chromatogr. A*, 1160, **2007**, 3.
19. J.C. Vire, A. Squella, J.M. Kauffmann, L.J. Nunez-Vergara, and G.J. Patriarche, *Anal. Lett*., 20, **1987**, 1467.
20. J.M. Kauffmann, J.C. Vire, G.J. Patriarche, L.J. Nunez-Vergara, and J.A. Squella, *Electrochim. Acta*, 32, **1987**, 1159.
21. L.J. Nunez-Vergara, J.A. Squella, K.L. Barnafi, J.C. Vire, J.M. Kauffmann, and G.J. Patriarche, *Anal. Lett.*, 19, **1986**, 2307.
22. D. Dogrukol-Ak, V. Zaimoglu, and M. Tuncel, *Eur. J. Pharm. Sci*., 7, **1999**, 215.
23. N. El-Enany, F. Belal, and M.S. Rizk, *J. Pharm Biomed. Anal*., 30, **2002**, 219.
24. R.N. Hegde and S.T. Nandibewoor, *ElectrodeAnal. Lett*., 41, **2008**, 977.
25. M.F. Yu, B.S. Files, S. Arepalli, and R.S. Ruoff, *Phys. Rev. Lett*., 84, **2000**, 5552.

26. E. Topoglidis, T. Lutz, R.L. Willis, C.J. Barnett, A.E.G. Cass, and J.R. Durrant, *Faraday. Discuss*., 116, **2000**, 35.
27. M.M. Collinson, H. Wang, R. Makote, and A. Khramov, *J. Electroanal. Chem.*, 519, **2002**, 65.
28. Q. Li, G. Luo, and J. Feng, *Electroanalysis*, 13, **2001**, 359.
29. C. Bittencourt, A. Felten, E.H. Espinosa, R. Ionescu, E. Liobet, X. Correig, and J.J. Pireaux, *Sensor Actuat. B*, 115, **2006**, 33.
30. B.Y. Wei, M.C. Hsu, H.M. Lin, R.J. Wu, and H.J. Lai, *Sensor. Actuat. B.*, 101, **2004**, 81.
31. Y. Chen, C. Zhu, and T. Wang, *Nanotechnology*, 17, **2006**, 3012.
32. G.J. Li and S. Kawi, *Mater. Lett.*, 34, **1998**, 99.
33. J. Xu, Q. Pan, Y. Shun, and Z. Tian, *Sensor. Actuat. B.*, 66, **2000**, 277.
34. H,Mahmoudi Moghaddam, H. Beitollahi, S. Tajik, I. Sheikhshoaie and P. Biparva, *Environ. Monit. Assess*., 187, **2015**, 1.
35. S.P. Kim and H.C. Choi, *Sens. Actuators B*, 207, **2015**, 424.
36. F. Wang, M. Xu, L. Wei, Y. Wei, Y. Hu, W. Fang, and C.G. Zhu, *Electrochim. Acta*, 153, **2015**, 170.
37. M. Kauf fmann, J.C. Vire, G.J. Patriarche, L.J. Nunez-Vergara, and J.A. Squella, *Electrochim. Acta*, 3, **1987**, 1159.
38. Y.Li and G. Shi, *J. Phys. Chem. B*, 109, **2005**, 23787.
39. R.N. Hegde, N.P. Shetti, and S.T. Nandibewoor, *Talanta*, 79, **2009**, 361.
40. D.K. Gosser, Cyclic Voltammetry: Simulation and Analysis of Reaction Mechanisms, VCH, (1993) New York, United States.
41. E. Laviron, *J. Electroanal. Chem*., 101, **1979**, 19.
42. A.J. Bard and L.R. Faulkner, Electrochemical Methods Fundamentals and Application, 2nd ed, Wiley, (2004) New York, United States.
43. M. Masui, H. Sayo, and Y. Tsuda, *J. Chem. Soc. B*, **1968**, 973